THE SHAPE OF UNSTABLE NUMERICAL SOLUTIONS OF INITIAL VALUE PROBLEMS

BY: R. Vichnevetsky *
H. Sandusky **

DCS-TR #44

*Department of Computer Science
Rutgers, The State University of New Jersey
New Brunswick, New Jersey 08903

**Department of Aerospace & Mechanical Sciences
Princeton University
Princeton, New Jersey 08540

Department of Computer Science
Rutgers University

May 1976

1. INTRODUCTION

We will analyze in this paper some properties of unstable solutions in the numerical approximation of partial differential equations of the initial value kind, with spatial variable x and time t. It is often, although incorrectly believed that numerical instability always manifests itself by the appearance of components which are oscillatory in time as well as space with a period near $2 \cdot \Delta t$ and a wavelength near $2 \cdot \Delta x$ i.e. of the kind illustrated in Fig. 1.

That this belief is widespread is probably due to the facts that:

a) this type of instability is the most common, and

b) simple examples in the classical literature tend to emphasize this type only.

But other types of numerical instability may and do occur. For instance, we demonstrate in §5 that instabilities of parabolic equations which grow exponentially in time rather than in an oscillatory manner exist with even-order accurate time-marching schemes. And in §6 we show that unstable solutions of hyperbolic equations have a wavelength of $4 \cdot \Delta x$, i.e. twice that of the parabolic case. We develop and illustrate these questions in detail by conducting an analysis in the frequency domain.

In §8, we comment upon the difference between the notions of step-wise and point-wise stability, and illustrate certain types of unstable solutions which occur despite the pointwise stability of the scheme.

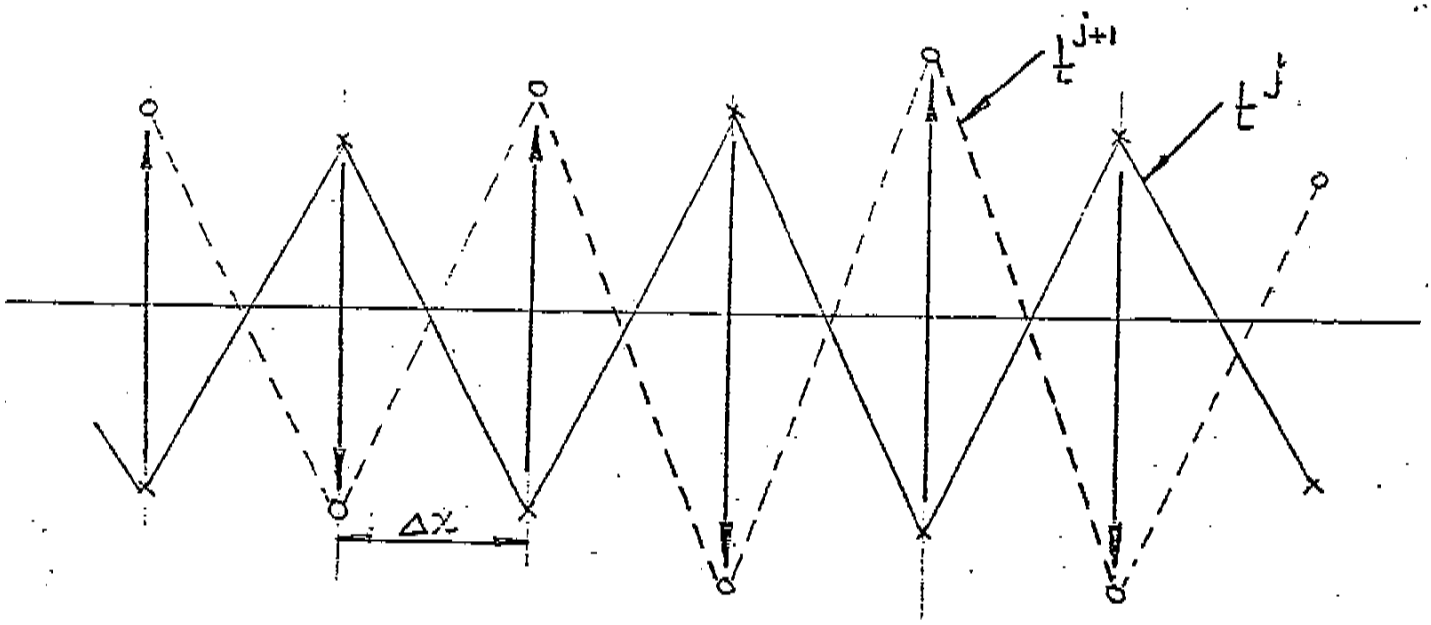

Figure 1 *Common type of oscillatory numerical instability. Period $\simeq 2.\Delta t$; Wavelength $\simeq 2 \cdot \Delta x$.*

2. THE HEAT EQUATION: I - OSCILLATORY INSTABILITY

Consider at first the simple heat equation

$$\frac{\partial u}{\partial t} = \sigma \frac{\partial^2 u}{\partial x^2} \tag{1}$$

approximated by the explicit scheme

$$\frac{u_n^{j+1} - u_n^j}{\Delta t} = \sigma \left(\frac{u_{n+1}^j + u_{n-1}^j - 2 u_n^j}{\Delta x^2} \right) \tag{2}$$

To analyse the numerical stability properties of this scheme, we consider the classical (Von Neumann) sinusoidal trial solutions

$$u_{\omega,n}^j = a_\omega^j \cdot e^{i \omega x_n} \tag{3}$$

which have the amplification factor

$$\frac{a_\omega^{j+1}}{a_\omega^j} = Z(\omega) = 1 + 2 \cdot \frac{\sigma \cdot \Delta t}{\Delta x^2} \left(\cos(\omega \cdot \Delta x) - 1 \right). \tag{4}$$

When

$$\frac{\sigma \cdot \Delta t}{\Delta x^2} > \frac{1}{2}, \tag{5}$$

then solutions of the form (3) corresponding to $\omega = \pi / \Delta x$ are unstable, with an oscillatory time behavior described by (4) with $Z(\omega)$ real, negative and larger than one in absolute value. This is the "classical" mode of instability illustrated in Fig. 1.

3. STABILITY CHARTS

To introduce flexibility in the analysis, we shall make use of stability charts of time-marching methods [6]. Their derivation is briefly outlined:

Numerical approximations of the general linear partial differential equation

$$\frac{\partial u}{\partial t} = X \cdot u \qquad (6)$$

may be viewed as obtained by

a] approximating the differential operator $X\cdot$ by a discrete approximation of the form

$$\frac{du_n}{dt} = A \cdot u_n , \qquad (7)$$

and,

b] approximating time-integration by a time-marching scheme

$$u_n^{j+1} = \mathbb{Z}(\Delta t \cdot A) \cdot u_n^j ,$$

where $\mathbb{Z}$ is a discrete operator, with coefficients containing $\Delta t \cdot A\cdot$ E.g., (2) is equivalent to first approximating (1) by central differences,

$$\frac{du_n}{dt} = A \cdot u_n \equiv \frac{\sigma}{\Delta x^2}\left(u_{n+1} + u_{n-1} - 2 \cdot u_n\right), \qquad (8)$$

and effecting then time-marching by Euler's explicit method

$$\mathbb{Z}(\Delta t \cdot A\cdot) = 1 + \Delta t \cdot A \cdot \qquad (9)$$

The following are then defined:

a) The complex function

$$\hat{A}(\omega) \equiv \frac{A \cdot e^{i\omega x_n}}{e^{i\omega x_n}} \qquad (10)$$

is defined as the *spectral function of the difference operator* A.

($\hat{A}(\omega) = -\frac{\sigma}{\Delta x^2}\left(2\cos(\omega\cdot\Delta x)-2\right)$ in the preceding example).

b) *Stability region of the time-marching method:*

For sinusoidal trial solutions of the form (3), the amplification factors may be expressed as

$$\frac{a_\omega^{j+1}}{a_\omega^j} = Z(\omega) = \mathcal{Z}\left(\Delta t \hat{A}(\omega)\right), \qquad (11)$$

obtained by simply replacing in (4) the operator A by its spectral function $\hat{A}(\omega)$.

Pointwise stability* requires that

$$|Z(\omega)| = |\mathcal{Z}(\Delta t \hat{A}(\omega))| \leq 1 \qquad (12)$$

for all ω.

To the stable region $|Z(\omega)| \leq 1$ corresponds a region S in the $\Delta t \hat{A}$ complex plane for which (12) holds, which is the *stability region* for the method of time-marching described by the operator $\mathcal{Z}$.

Its boundary ∂S is the set of points in the $\Delta t \hat{A}$ plane for which $|Z(\omega)| = 1$ or $Z(\omega) = e^{i\alpha}$ (α real). These points correspond to amplitude conservative sinusoidal solutions, and the value of α describes their phase displacement per time step:

$$u_{\omega,n}^{j+1} = e^{i\alpha} \cdot u_{\omega,n}^{j}$$

$$= a_\omega^j \, e^{i(\omega x_n + \alpha)} \qquad (13)$$

*See e.g. Hildebrand (1968) pp. 143 *et seq.* for a definition of pointwise and stepwise numerical stability.

E.g., the stability boundary ∂S shown for Euler's explicit method in Fig. 2 is the circle of radius 1 and center (-1,0); the stability region S is the disk interior to that circle.

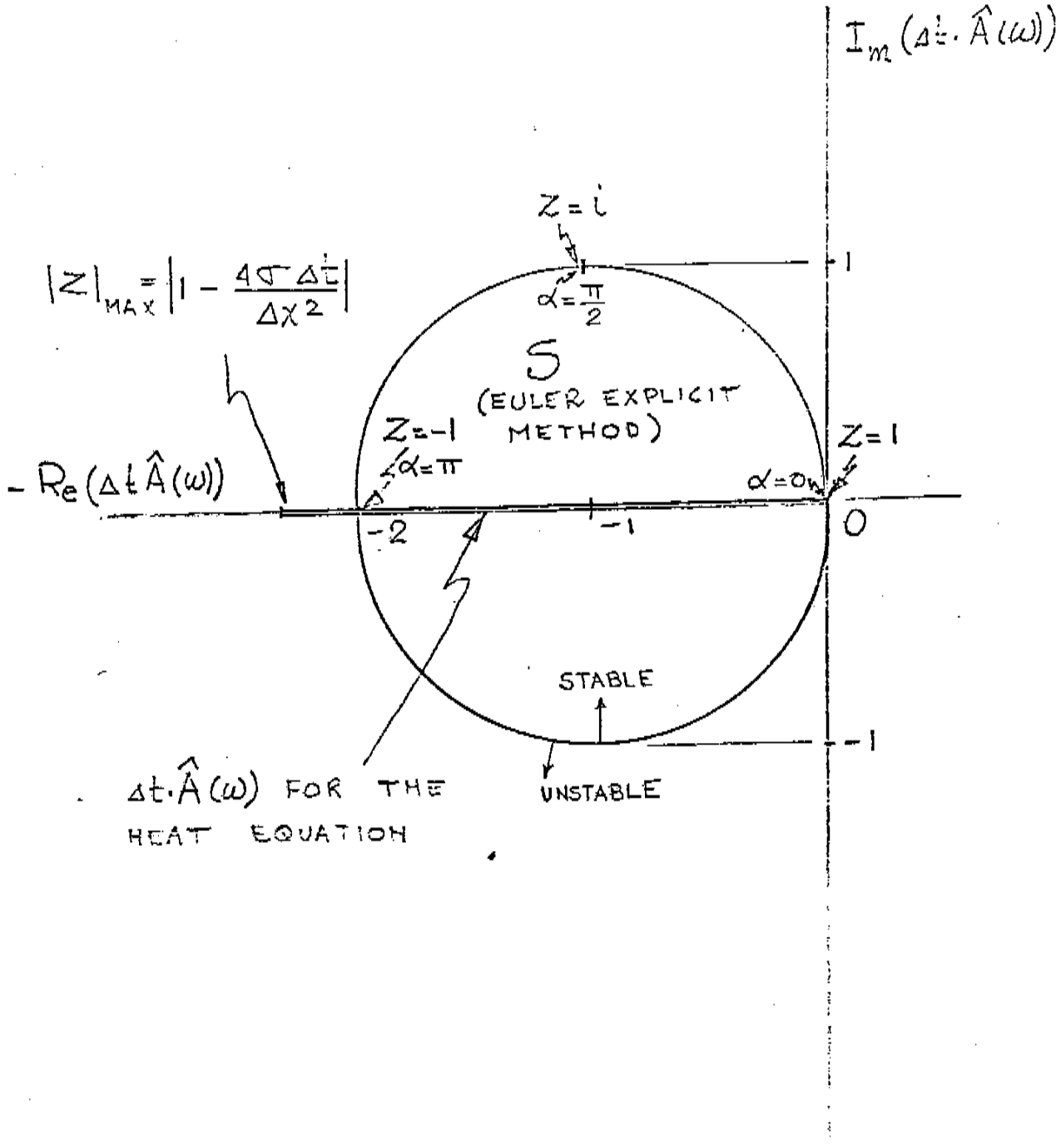

Figure 2 *The point $|Z|_{max}$ on the real negative axis corresponds to $\omega \cdot \Delta x = \pi$ When instability occurs, it corresponds to real negative values of Z (less than -1).*

4. DOMINANT MODE OF INSTABILITY

When instability occurs, the shape of unstable solutions is close to that of the *dominant mode*, i.e. that of the sinusoidal solution for which $|Z(\omega)|$ is the maximum. Indeed, this mode quickly overshadows all other ones.

Returning to our previous example, (in § 2) we have:

a) $\hat{A}(\omega)$ is real non-positive for all values of ω

b) The only way in which $\Delta t \cdot \hat{A}(\omega)$ may lie outside of S for Euler's explicit method is when

$$\left|\Delta t\, \hat{A}(\omega)\right|_{max} = 4 \cdot \frac{\sigma \cdot \Delta t}{\Delta x^2} > 2 \qquad (14)$$

The dominant mode corresponds to $\omega = \pi/\Delta x$ and $\alpha = \pi$, which generates precisely the type of instability illustrated in Fig. 1.

5. THE HEAT EQUATION: II-MONOTONIC INSTABILITY

Suppose now that we were to integrate (8) in time by the explicit method with second order accuracy:

$$\left.\begin{aligned} u_n^{j+\frac{1}{2}} &= u_n^j + (\Delta t \cdot A \cdot u_n^j)/2 \\ u_n^{j+1} &= u_n^j + \Delta t \cdot A \cdot u_n^{j+\frac{1}{2}} \end{aligned}\right\} \qquad (15)$$

instead of by Euler's explicit method.

The operator $\mathbb{Z}$ for this method is

$$\mathbb{Z} = 1 + \Delta t A \cdot + (\Delta t \cdot A \cdot)^2/2 \qquad (16)$$

i.e. $$Z(\omega) = 1 + \Delta t \hat{A}(\omega) + (\Delta t \cdot \hat{A}(\omega))^2/2 \qquad (16-2)$$

and the stability region is that shown in Fig. 3. It may be seen that numerical instability will also occur when (5) is violated, with a

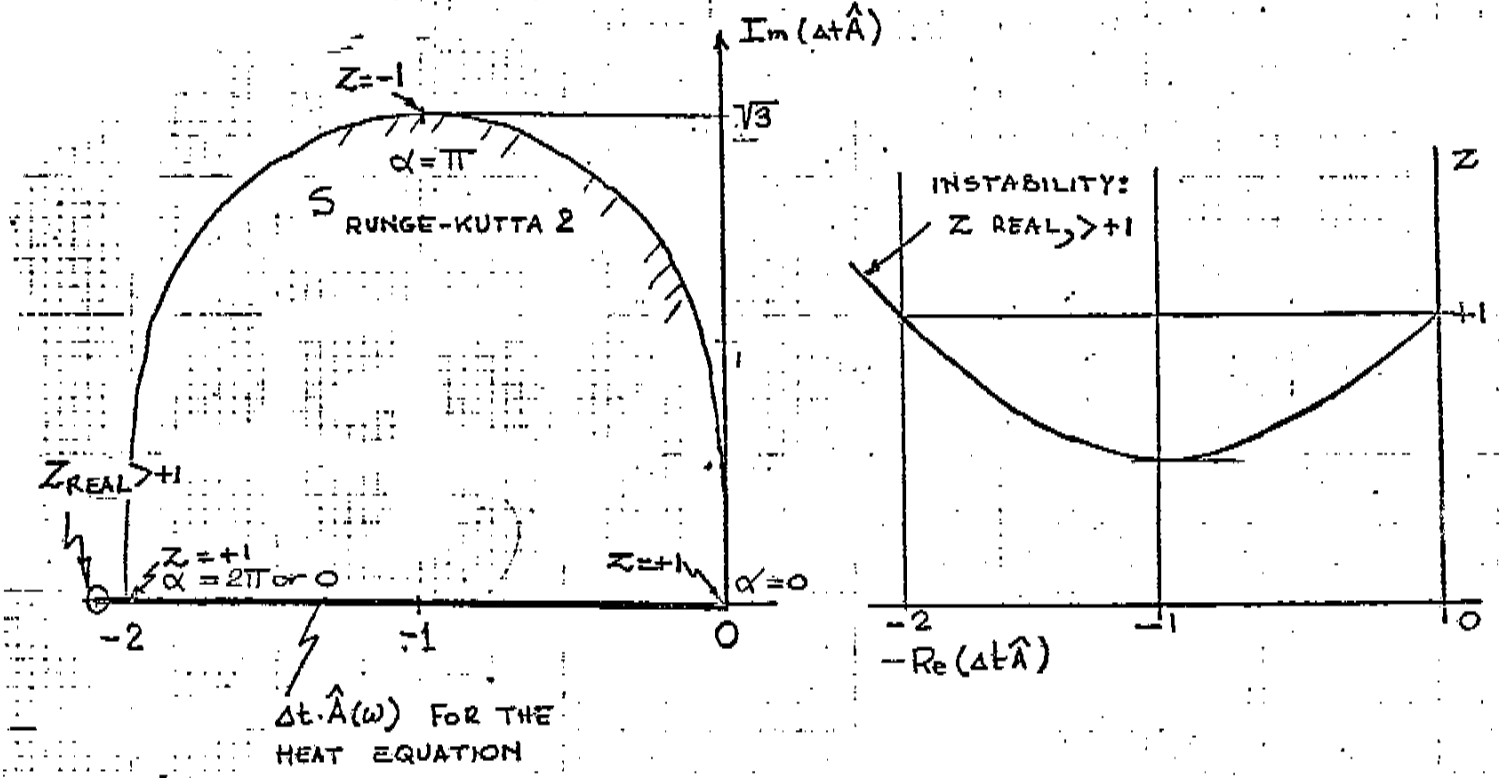

Fig 3

dominant value $Z\left(\frac{\pi}{\Delta x}\right)$ which is now positive real, larger than +1, (instead of negative, real, less than -1). The corresponding instability has the monotonic type of behavior illustrated in Fig. 4. We shall call the case: (Z real, $<$ -1) *oscillatory instability* and the case: (Z real, $>$ +1) *monotonic instability*.

Both are strictly related to the method of time marching, and *disappear when* Δt *is reduced so as to satisfy the stability condition (5),* which happens to be common to both.

It is easily demonstrated that monotonic instability will occur whenever time marching is effected with an even order accurate method (for the heat equation) and oscillatory instability with odd order methods.

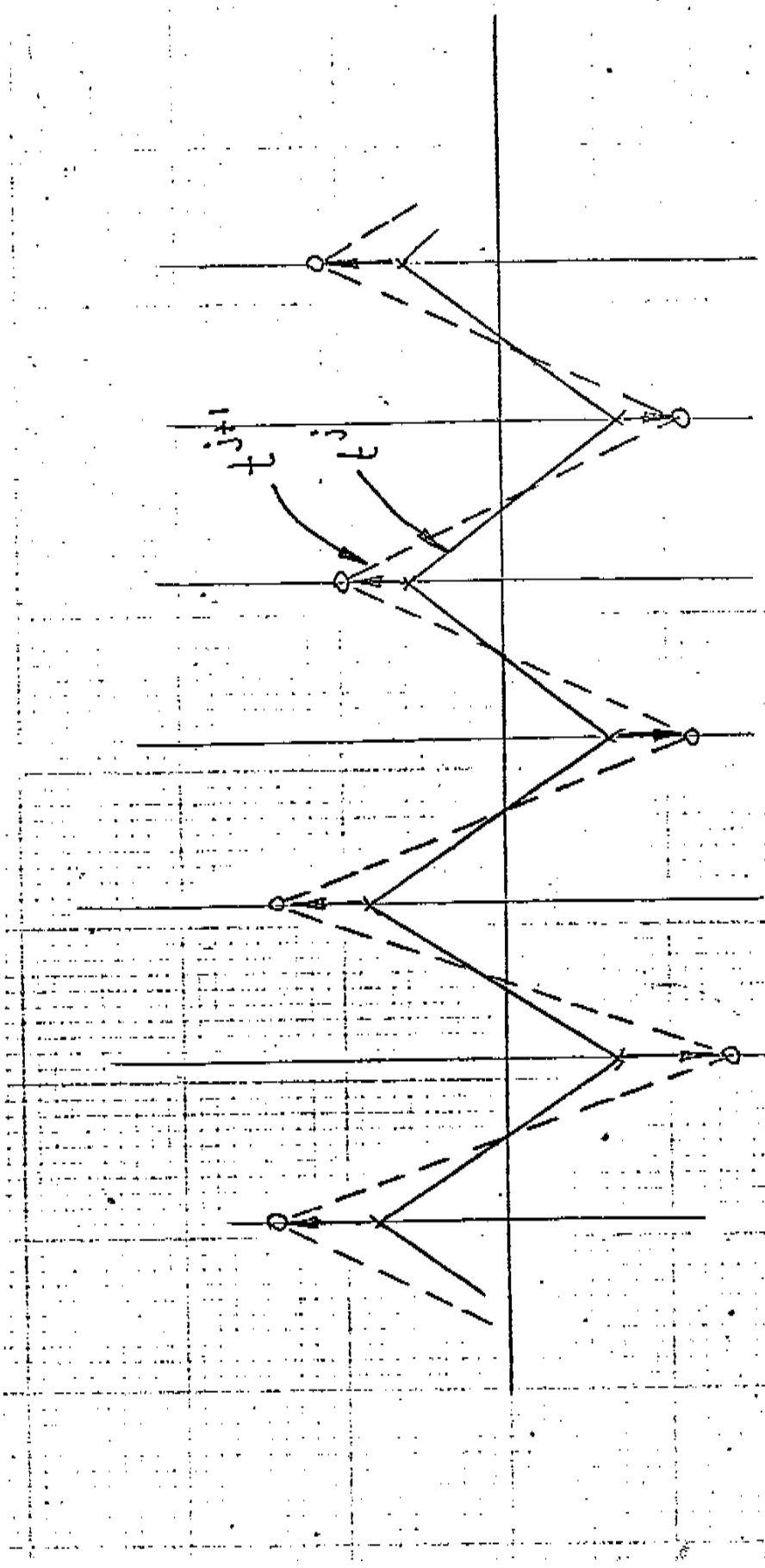

Fig 4.

6. INSTABILITY WITH THE LEAPFROG METHOD FOR HYPERBOLIC EQUATIONS

We shall show that other types of instabilities, different in behavior from those indentified so far, can also occur.

Consider the simple advection equation

$$\frac{\partial u}{\partial t} + c\frac{\partial u}{\partial x} = 0 \tag{17}$$

approximated by the semi-discretization obtained by simple central differences:

$$\frac{du_n}{dt} = -c\left(\frac{u_{n+1} - u_{n-1}}{2\cdot\Delta x}\right) \equiv A\cdot u_n \tag{18}$$

and integrated in time by the leapfrog method:

$$u_n^{j+1} = u_n^{j-1} + 2\cdot\Delta t\cdot A\cdot u_n^j \tag{19}$$

The spectral function

$$\hat{A}(\omega) = \frac{A\cdot e^{i\omega x_n}}{e^{i\omega x_n}} = \frac{-i\cdot c\cdot \sin(\omega\cdot\Delta x)}{\Delta x} \tag{20}$$

is pure imaginary for all ω, and the time-marching method (19) is stepwise stable (and conservative) if the Courant-Friedrichs-Lewy condition

$$\left|\frac{c\cdot\Delta t}{\Delta x}\right| \leq 1 \tag{21}$$

is satisfied.

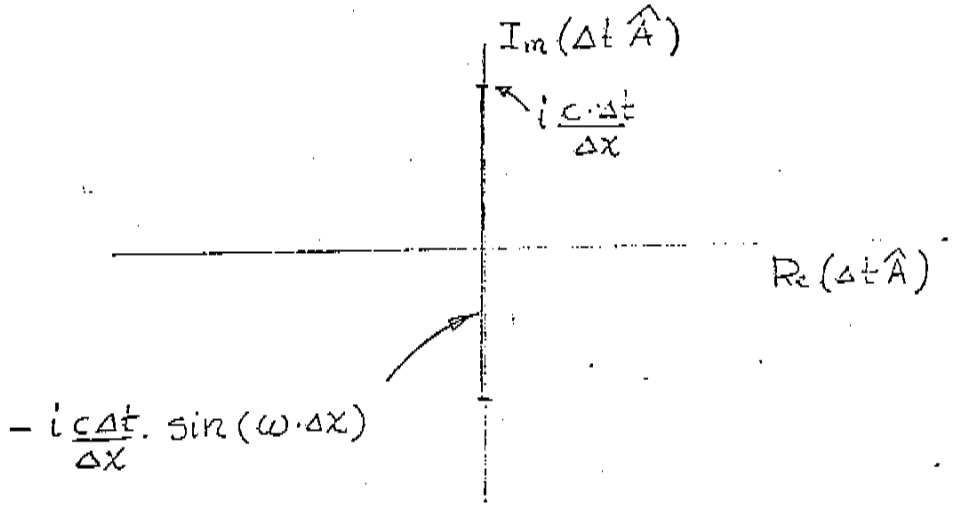

Figure 5

Spectral function $\Delta t\cdot\hat{A}(\omega)$ for the advection (hyperbolic) equation discretized in space as (18).

We note that the maximum of $\Delta t\cdot\hat{A}(\omega)$ occurs for $\omega=\frac{\pi}{2\cdot\Delta x}$ (wavelength $=4\cdot\Delta x$):

$$\Delta t\cdot\hat{A}\left(\frac{\pi}{2\cdot\Delta x}\right)=-i\,\frac{c\cdot\Delta t}{\Delta x} \tag{22}$$

To analyse the time behavior of the corresponding dominant mode, we write from (19):

$$\left(a^{j+1}-2\cdot\Delta t\cdot\left(-i\,\frac{c}{\Delta x}\right)\cdot a^{j}-a^{j-1}\right)e^{i\omega x_n}=0 \tag{23}$$

or

$$z^2+2\cdot\Delta t\left(i\,\frac{c}{\Delta x}\right)\cdot z-1=0 \tag{24}$$

whence,

$$Z = \frac{a^{j+1}}{a^j} = -i\frac{c\cdot\Delta t}{\Delta x} \pm \sqrt{-\left(\frac{c\Delta t}{\Delta x}\right)^2 + 1} \qquad (25)$$

which is complex and of unity amplitude when $\left|\frac{c\cdot\Delta t}{\Delta x}\right| \leq 1$

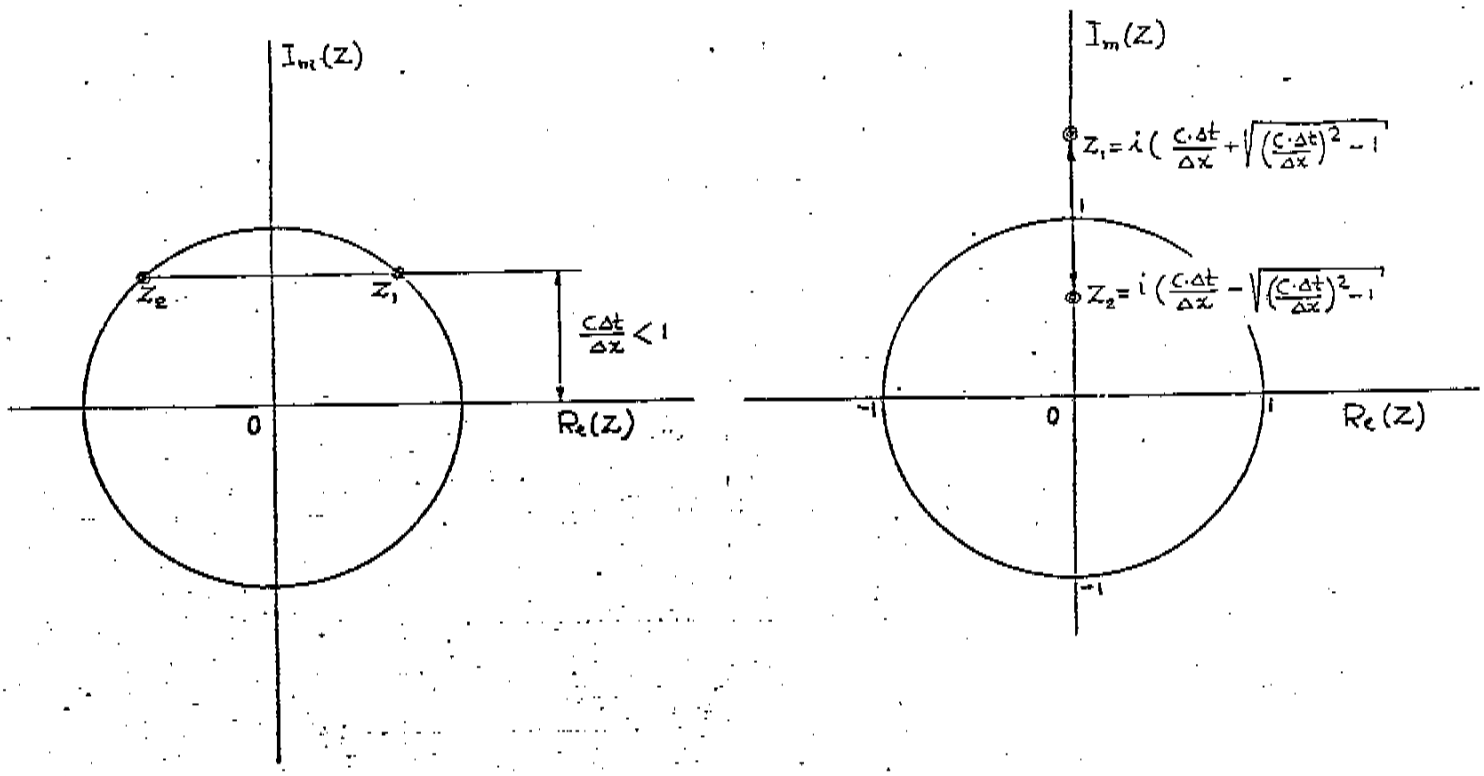

Figure 6

Amplification factors for $\omega = \pi/(2\cdot\Delta x)$.

(a) $(c\cdot\Delta t/\Delta x) < 1$: *the amplification factors* $|Z_1|$ *and* $|Z_2|$ *equal 1.*

(b) $c\Delta t/\Delta x > 1$: *One of the amplification factors* $|Z_1|$ *is larger than 1.*

Instability occurs when the term under the radical becomes negative, and Z then becomes pure-imaginary with one of the two roots in (25) of amplitude greater than one. The dominant mode of instability's behavior is illustrated in Fig. 7.

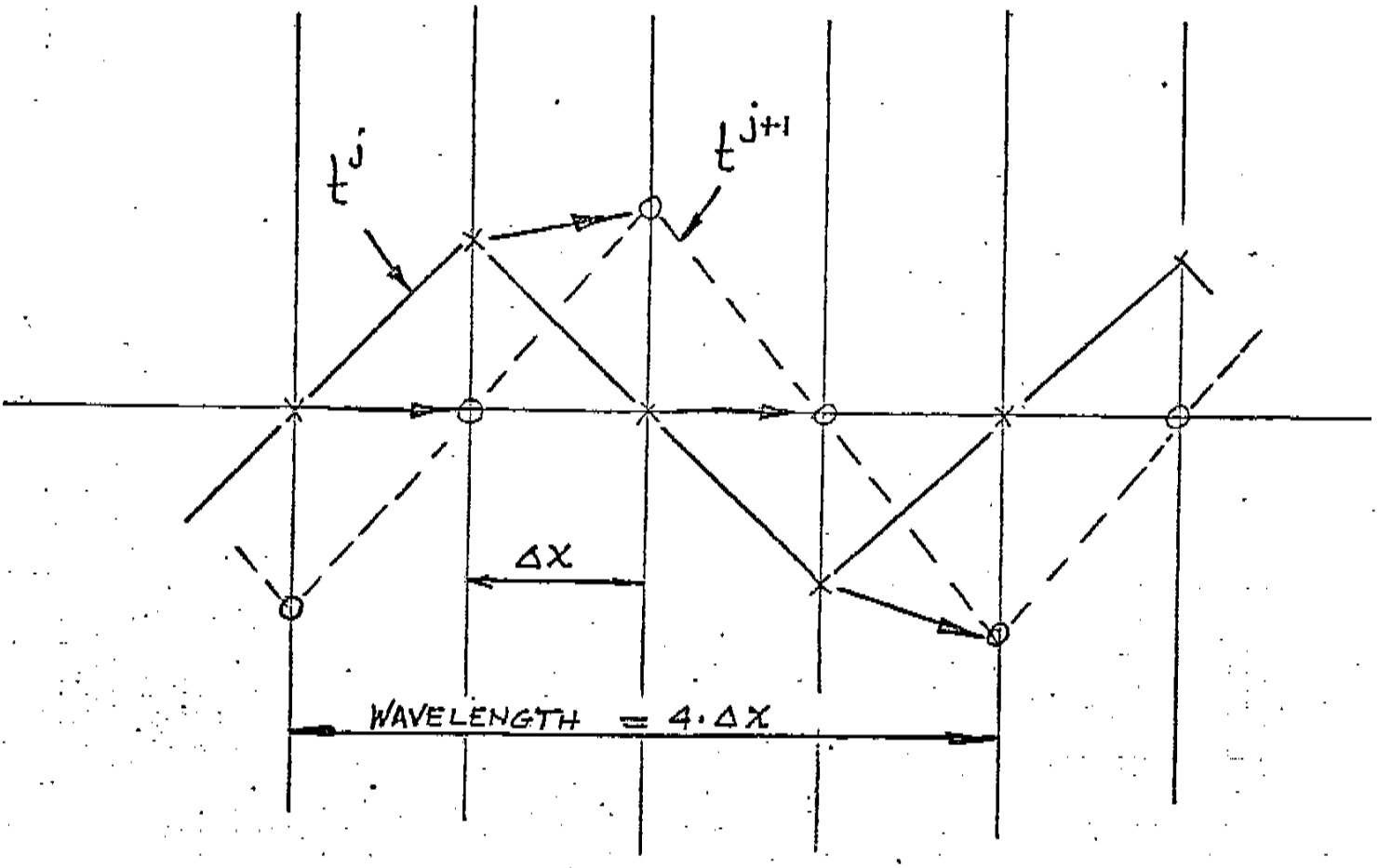

Figure 7

Numerical instability with the advection (hyperbolic) equation integrated in time by the leapfrog method (wavelength = $4 \cdot \Delta X$; velocity = $\Delta X / \Delta t$)

This instability differs from those previously analysed in two important respects:

- first, the wavelength of the dominant unstable mode is not $2 \cdot \Delta X$ as before, but is twice as much, i.e. $\underline{4 \cdot \Delta X}$.

- second, the growth is not oscillatory, but is closer to the monotonic instability of the parabolic equation studied before, with the added fact that there is translation,

The unstable solution of wavelength $4.\Delta x$ illustrated in Fig. 7 has the phase velocity $c^* = \frac{\Delta x}{\Delta t}$ which is less than c, but independent of it. This is the largest velocity at which numerical data can be propagated with the given method in the computing mesh of size $(\Delta x, \Delta t)$. Instability in this case occurs when the mesh structure prevents the solution to travel at the velocity c but limits it to the velocity $c^* = \frac{\Delta x}{\Delta t} < c$: instead of moving fast enough, the numerical solution grows in amplitude.

7. ANOTHER EXAMPLE: THE ADVECTION-DIFFUSION EQUATION

Our next example illustrates the fact that all three of the types of instability thus far described can occur within a given computing scheme merely by changing the mesh size and/or parameters of the equation.

Consider the linear advection-diffusion equation:

$$\frac{\partial u}{\partial t} = -c\,\frac{\partial u}{\partial x} + \sigma\,\frac{\partial^2 u}{\partial x^2} - k\cdot u \qquad (26)$$

semi-discretized as:

$$\frac{du_n}{dt} = -c\left[\frac{u_{n+1} - u_{n-1}}{2\cdot\Delta x}\right] + \sigma\left[\frac{u_{n+1} + u_{n-1} - 2\cdot u_n}{\Delta x^2}\right] - k\cdot u_n \equiv A\cdot u_n \qquad (27)$$

The spectral function of the operator $A\cdot$ is:

$$\hat{A}(\omega) \equiv \frac{A\cdot e^{i\omega x_n}}{e^{i\omega x_n}} = -ic\cdot\frac{\sin(\omega\cdot\Delta x)}{\Delta x} - \frac{4\cdot\sigma}{\Delta x^2}\cdot\sin^2\left(\frac{\omega\cdot\Delta x}{2}\right) - k \qquad (28)$$

It is the equation of the ellipse illustrated in Fig. 8.

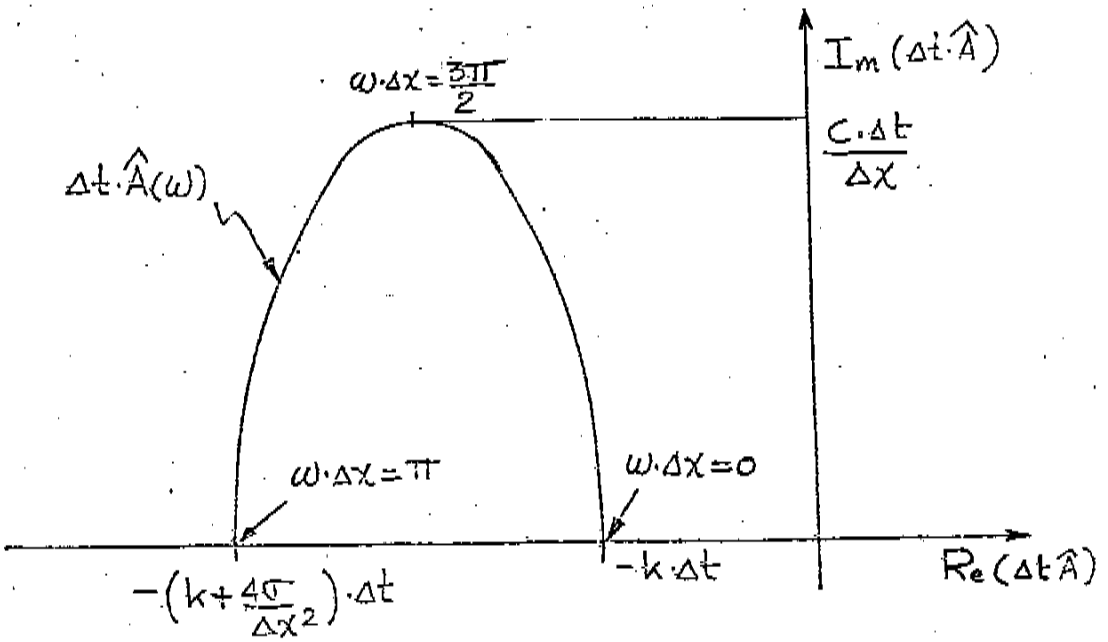

Figure 8 - Spectral function of the semi-discretization (26) of the advection-diffusion equation.

Consider now the time-integration of (26) by Euler's explicit method. Illustrated in Fig. 9 are the spectral functions $\Delta t \cdot \hat{A}(\omega)$ for three different combinations of the parameters $c, \sigma, k, \Delta x$ and Δt superimposed on the stability boundary S for time-integration by Euler's explicit method.

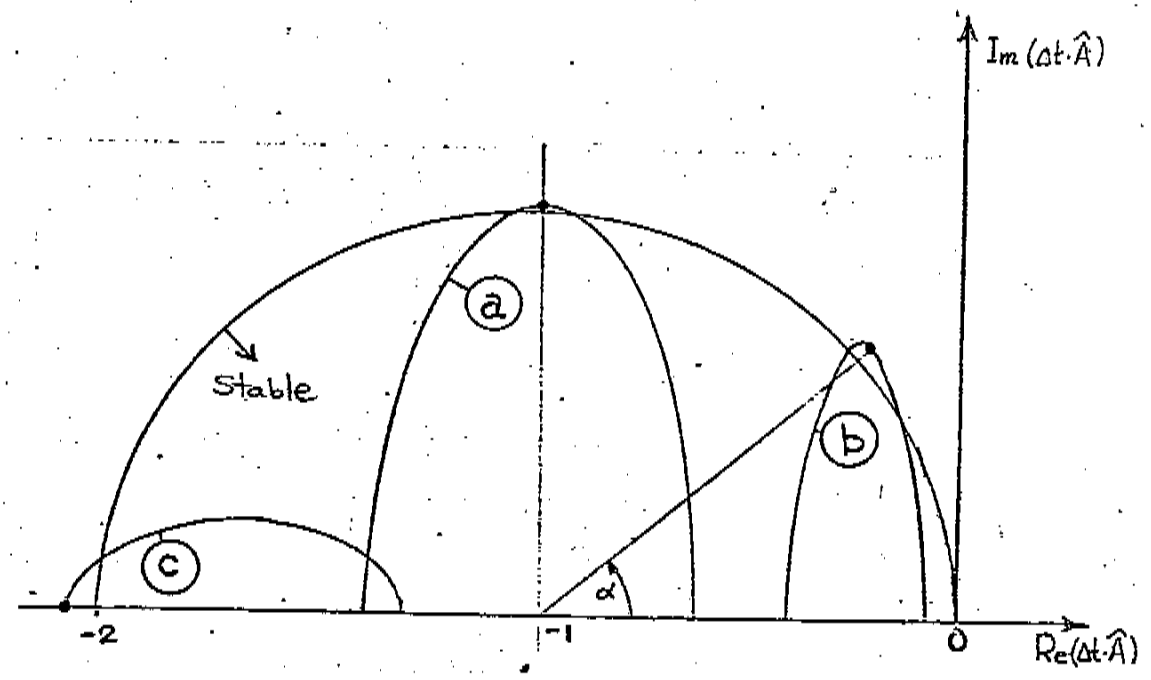

Figure 9

The following analyses refer to the cases a), b) and c) illustrated in Fig. 9. In each case, the *dominant mode* of instability is that corresponding to the value of ω for which $|Z(\omega)|$ is maximum, i.e. for which $\Delta t\,\hat{A}(\omega)$ lies the furthest outside of S. In all three cases the instability disappears when Δt is reduced,

Case a)

The dominant mode of instability occurs at or near $\omega \cdot \Delta x = -\pi/2$ (wavelength = $4 \cdot \Delta x$) with a time behavior described by:

$$Z(\omega) = (1+\varepsilon) \cdot e^{i\pi/2} = i\,(1+\varepsilon)$$
$$(\varepsilon > 0)$$

This corresponds to an increase in amplitude and a phase shift of one-quarter wavelength (Δx) per time step, i.e. a velocity equal to $\Delta x/\Delta t$ (as illustrated before in Fig. 7).

Case b)

The dominant mode of numerical instability occurs again for $\omega \simeq \pi/2 \cdot \Delta x$, i.e. for sinusoidal components of wavelength near $4 \cdot \Delta x$. The corresponding amplification factor is (from Fig. 9)

$$Z\left(\frac{\pi}{2 \cdot \Delta x}\right) = (1+\varepsilon)\, e^{i\alpha}$$
$$0 < \alpha < \pi/2$$

As shown in Fig. 10, the phase shift per time-step is now less than the $\frac{\pi}{2}$ value of case a).

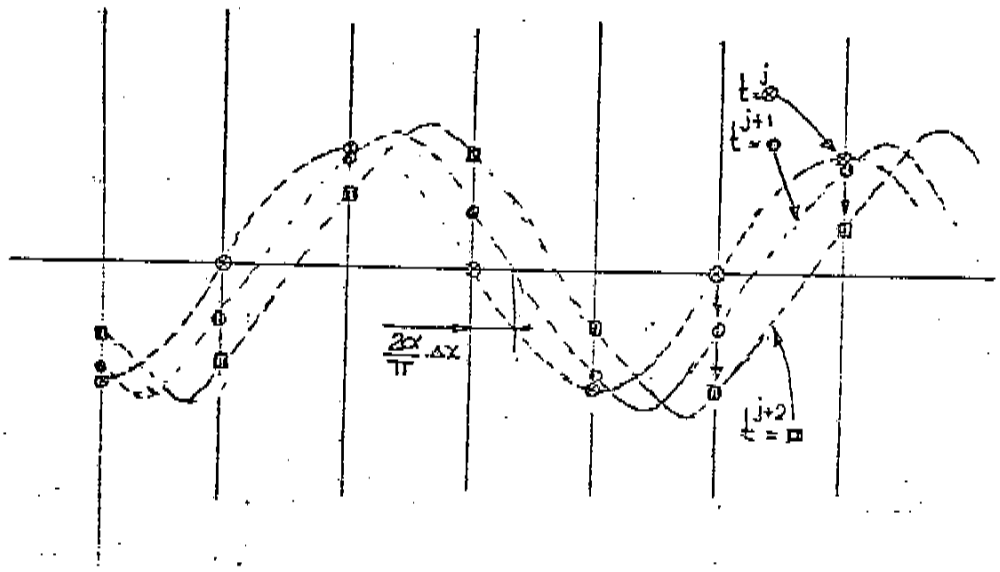

Figure 10 - The dominant unstable error mode is of wavelength $\simeq 4 \cdot \Delta x$, *and moves at the velocity* $(2 \cdot \alpha \cdot \Delta x)/(\pi \cdot \Delta t)$

In <u>case c</u>, the dominant mode of instability occurs for $\omega = \pi/\Delta x$. This corresponds to the common type of instability illustrated for the parabolic equation in Fig. 1.

8. GENERIC INSTABILITY

Consider now the simple advection equation (17) approximated by the semi-discretization (18), and integrated in time by Euler's explicit method:

$$\frac{u_n^{j+1} - u_n^j}{\Delta t} = -\frac{c \cdot \Delta t}{\Delta x}\left(\frac{u_{n+1}^j - u_{n-1}^j}{2 \cdot \Delta x}\right) \equiv A \cdot u_n^j \qquad (30)$$

This combination is always stepwise unstable, since the spectral function

$$\hat{A}(\omega) = -i\,\frac{c \cdot \Delta t}{\Delta x} \cdot \sin(\omega \cdot \Delta x) \qquad (31)$$

is pure imaginary, whereas the stability region S for Euler's method excludes the imaginary axis of the complex plane as shown in Fig. 11.

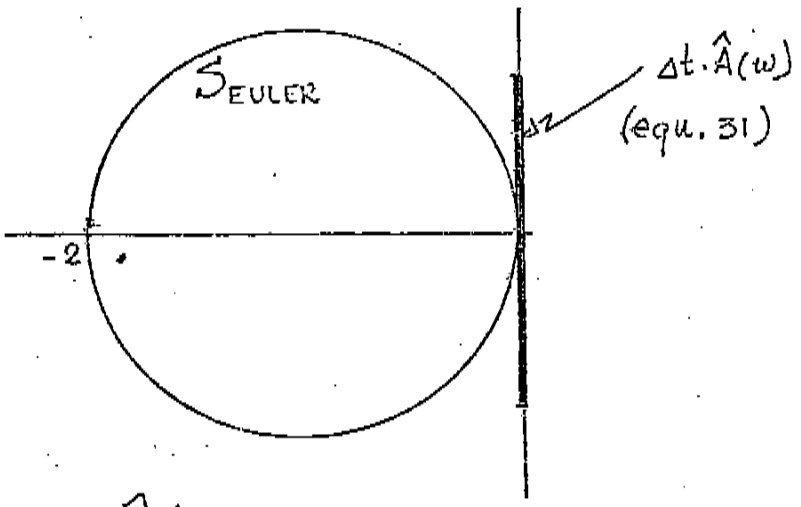

Figure 11 - The spectral function $\hat{A}(\omega)$ for the advection equation lies outside of the stability region S of Euler's explicit time marching-method.

The amplification factor:

$$Z(\omega) = 1 - i \frac{c \cdot \Delta t}{\Delta x} \cdot \sin(\omega \cdot \Delta x) \qquad (32)$$

has a real part which is always positive. The growth in time of sinusoidal terms is qualitatively similar to that illustrated in Fig. 10.

The components of wavelength $2 \cdot \Delta x$ have the interesting property of remaining invariant (no change in amplitude nor phase from t^j to t^{j+1}) but components at all other frequencies grow in amplitude as

$$|Z(\omega)| = \sqrt{1 + \left(\frac{c \cdot \Delta t}{\Delta x} \cdot \sin(\omega \cdot \Delta x)\right)^2}$$

$$= 1 + \frac{1}{2}\left(\frac{c \cdot \Delta t}{\Delta x} \cdot \sin(\omega \cdot \Delta x)\right)^2 + \cdots$$

$$= 1 + O(\Delta t^2), \qquad (33)$$

moving in phase by

$$\angle Z(\omega) = \arctan\left(\frac{c \cdot \Delta t}{\Delta x} \cdot \sin(\omega \cdot \Delta x)\right) \qquad (34)$$

at each time step, This corresponds to a velocity of displacement:

$$c^*(\omega) = \frac{\angle Z(\omega)}{\omega \cdot \Delta t} = \frac{1}{\omega \cdot \Delta t} \cdot \arctan\left(\frac{c \cdot \Delta t}{\Delta x} \cdot \sin(\omega \cdot \Delta x)\right) \qquad (35)$$

which, for $\omega \to 0$ is consistent:

$$\lim_{\omega \to 0} c^*(\omega) = c$$

The dominant mode occurs for $\omega = \pi/(2 \cdot \Delta x)$ for which the wavelength is $4 \cdot \Delta x$ For this dominant mode, the amplification per time-step is:

$$|Z\left(\frac{\pi}{2 \cdot \Delta x}\right)| = \sqrt{1 + \left(\frac{c \cdot \Delta t}{\Delta x}\right)^2} \qquad (36)$$

and the velocity of displacement is:

$$c^*\left(\frac{\pi}{2 \cdot \Delta x}\right) = \frac{2 \cdot \Delta x}{\pi \cdot \Delta t} \cdot \arctan\left(\frac{c \cdot \Delta t}{\Delta x}\right) \qquad (37)$$

It satisfies:

$$\frac{\Delta x}{2 \cdot \Delta t} \leq c^*\left(\frac{\pi}{2 \cdot \Delta x}\right) < \frac{\Delta x}{\Delta t} \qquad (38)$$

That components of all frequencies are stepwise unstable must be construed as due to a bad choice of the time-marching method, while the instabilities of all previously studied cases in this chapter were due to too large a choice of Δt.

The Pointwise Stability and Convergence

Pointwise stability of (30) is a more delicate question: one must define a relation of the form

$$\Delta x = g(\Delta t) \tag{39}$$

which forces Δx to go to zero simultaneously with Δt :

$$\Delta t = T/J \quad \text{as} \quad J \to \infty$$

Pointwise stability exists if the Von Neumann condition:

$$\lim_{\Delta t \to 0} |Z| \leq 1 + O(\Delta t) \tag{40}$$

is satisfied within this limiting process.

We have from (36) for small Courant number $\left(\frac{c \cdot \Delta t}{\Delta x}\right)$:

$$|Z|_{max} = \left|Z\left(\frac{\pi}{2 \cdot \Delta x}\right)\right| \simeq 1 + \frac{1}{2}\left(\frac{c \cdot \Delta t}{\Delta x}\right)^2$$

To have this quantity satisfy the Von Neumann condition (40) requires that $(\Delta t / \Delta x)^2 \to 0$ at least as $O(\Delta t)$. This can be achieved for instance, by letting $(\Delta t / \Delta x^2)$ = constant, i.e.

$$\Delta x = g(\Delta t) = \text{constant} * \sqrt{\Delta t} \tag{41}$$

In this sense, one can construct a family of computations with the algorithm (30) whose solution will converge to the exact solution as $\Delta t \to 0$. It is interesting to note that in this process, the Courant number goes to zero with Δt ; if it were to be implemented, the calculation would presumably tend to be extremely costly.

This illustrates the gap that exists between theoretical and practical approaches to a same problem. To a theorist (30) is a perfectly acceptable numerical approximation of the advection equation, since, if $(\Delta t/\Delta x^2)$ is kept constant, then

$$\exists\, \Delta t \ni \| u^T - u(x,T) \| < \varepsilon \;\forall\; \varepsilon > 0$$

(abstract notation intended!).

To the practitioner, pointwise growth of error for a fixed Δt is growth of error, i.e. instability. That the Von Neumann sufficient condition for pointwise stability may be satisfied is of little use to him, and that a small enough Δt and Δx would bring the error within specified bounds may be well beyond what he wants to or can afford in terms of machine-computational effort. *While pointwise stable*, the method is stepwise unstable.*

*that is if the rule $(\Delta t/\Delta x^2)$ = constant is used

We note in passing that this case is called "static instability" by Roache* (for reasons that are not clear to us) as opposed to the oscillatory instability (6), which he calls "dynamic instability." We prefer to use the word *generic* to define the type of instability identified here.

*Roache, P.J. (1972), Computational Fluid Dynamics. Hermosa Publishers, pg. 34. The terms "oscillatory" and "monotonic" instabilities used before were suggested by the partial analysis found in this book. The type of instability of § 5 which is also monotonic, but due to a large Δt rather than to a bad choice of method is not mentioned by Roache.

8. ANOTHER CASE OF GENERIC INSTABILITY: THE DESTABILIZING EFFECT OF DISSIPATIVE TERMS IN THE LEAPFROG METHOD FOR HYPERBOLIC EQUATIONS.

Consider the addition of a small dissipative term to the advection equation (12):

$$\frac{\partial u}{\partial t} = -c\,\frac{\partial u}{\partial x} - k\cdot u \qquad (42)$$

Physically, the term $-k.u$ has a stabilizing effect on solutions of the exact equation: sinusoidal terms have the exact behavior

$$u_\omega(x,t) = a_\omega(0)\cdot e^{-k\cdot t}\cdot e^{i\omega(x-ct)} \qquad (43)$$

whose amplitude decreases exponentially in time.

When semi-discretization and marching are effected as above (central differences in space and leapfrog in time), then the $(-ku)$ term has numerically the opposite effect: the method becomes unstable. That this be the case may be inferred without much analysis from the consideration of stability regions:

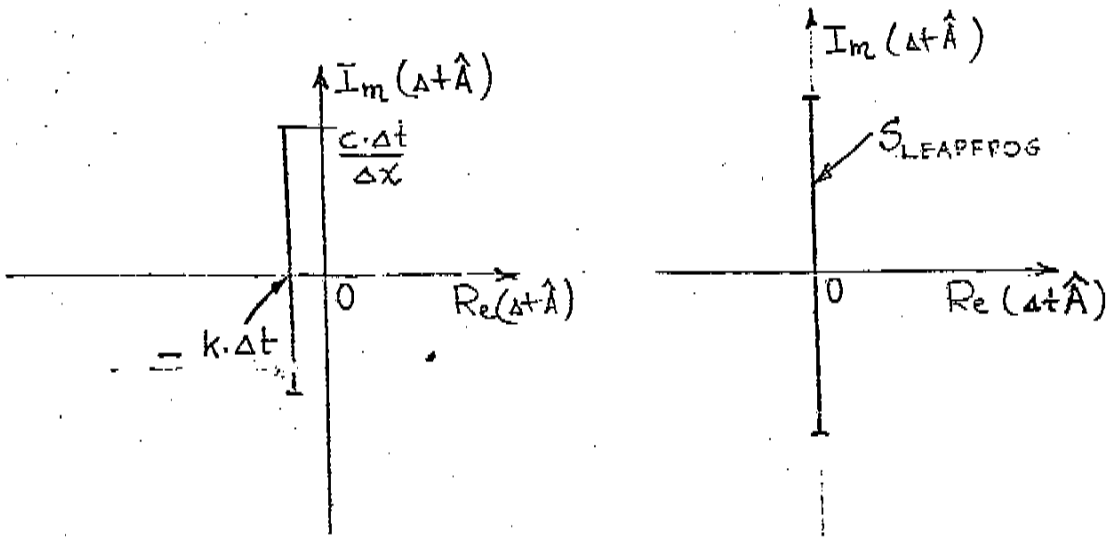

Figure 12 - The spectral function $\Delta t\,\hat{A}$ is outside of S for the leapfrog method of time-marching.

Without going into an extensive analysis, one may find out what the unstable solution will look like. Fig. 13 shows that with small values of k the line $\Delta t\hat{A}(\omega)$ is near S, thus the unstable values of z (for all ω) will be near (but outside) the circle $|z|=1$. This is illustrated in the following figure:

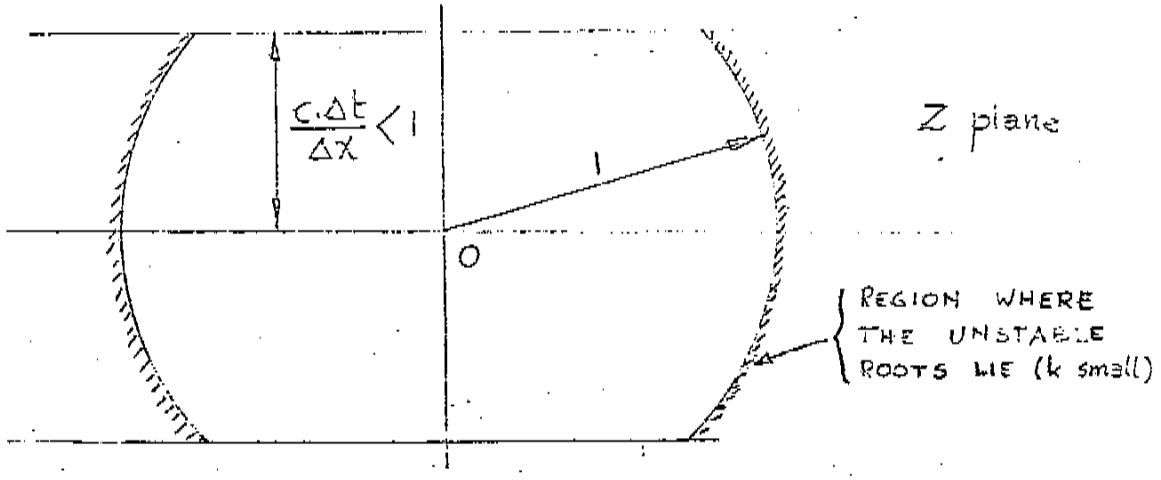

Figure 13

The corresponding solutions assume a sinusoidal shape similar to the stable case in terms of phase velocity, (at all frequencies ω), but with amplitudes that grow as* (for constant values of $\frac{c\cdot\Delta t}{\Delta x}<1$):

$$\left|\frac{a_\omega^{j+1}}{a_\omega^j}\right| = |z(\omega)| = 1+\beta\cdot k\cdot\Delta t \qquad (44)$$

where β is a finite, positive number. They generally resemble those illustrated in figure 10.

*this result is easily obtained by replacing $\left(i\frac{c\cdot\Delta t}{\Delta x}\right)$ by $\left(-k+i\frac{c}{\Delta x}\right)\cdot\Delta t$ in (24') and solving for z. Expanding the result in Taylor Series when $\Delta t\to 0$ with constant Courant number then yields (44).

This is also a border case which is stepwise unstable, while the Von Neumann condition for pointwise stability is satisfied:

$$|z| \leq 1 + O(\Delta t) \tag{45}$$

As in the previous example, that this condition is satisfied can have theoretical merits, but is of little interest to the programmer who wants to find a practical method to compute numerical solutions of the dissipative advection equation (40).

9. COMPUTER EXPERIMENTS

Several computer experiments have been done to verify the theory just presented. They all correspond to numerical integrations of the advection-diffusion equation approximated by (27) and integrated in time by Euler's explicit method. The choice of parameters corresponds to the cases labeled a), b) and c) in Fig. 9, and the initial condition of the calculation was that corresponding to steady state (where the solution should rest if no numerical instability did occur). With the constant boundary conditions :

$$u(0,t) = 1 \quad ; \quad \frac{\partial u}{\partial x}(\infty, t) = 0$$

the steady state solution is

$$u^{\circ}(x) = e^{-\lambda x} \tag{46}$$

with

$$\lambda = \frac{\sqrt{c^2 + 4\sigma k} - c}{2\sigma}$$

Fig 14. a), b) and c) illustrate the occurence of the three types of instability predicted by the theory.

Figure 14a

This instability, corresponding to a) in Fig. 9, has a wavelength of $4 \cdot \Delta x$ and a period of $4 \cdot \Delta t$.

Figure 14b

This instability, corresponding to b) in Fig. 9, has a wavelength near $4 \cdot \Delta x$ and a period near $8 \cdot \Delta t$.

Figure 14c

This instability, corresponding to c) in Fig. 9, has a wavelength of $2 \cdot \Delta x$ and a period of $2 \cdot \Delta t$ (the classical type of instability.)

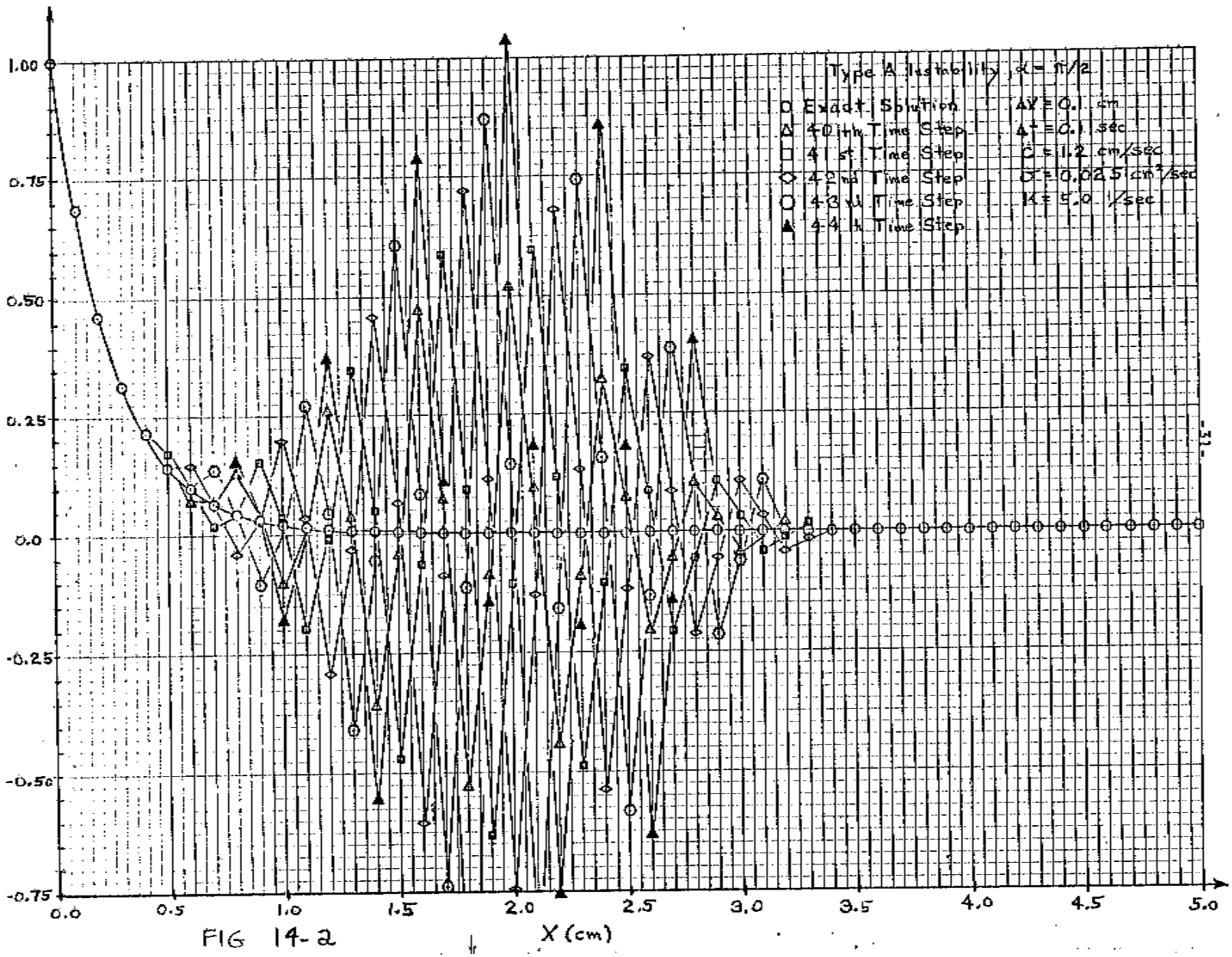

FIG 14-2

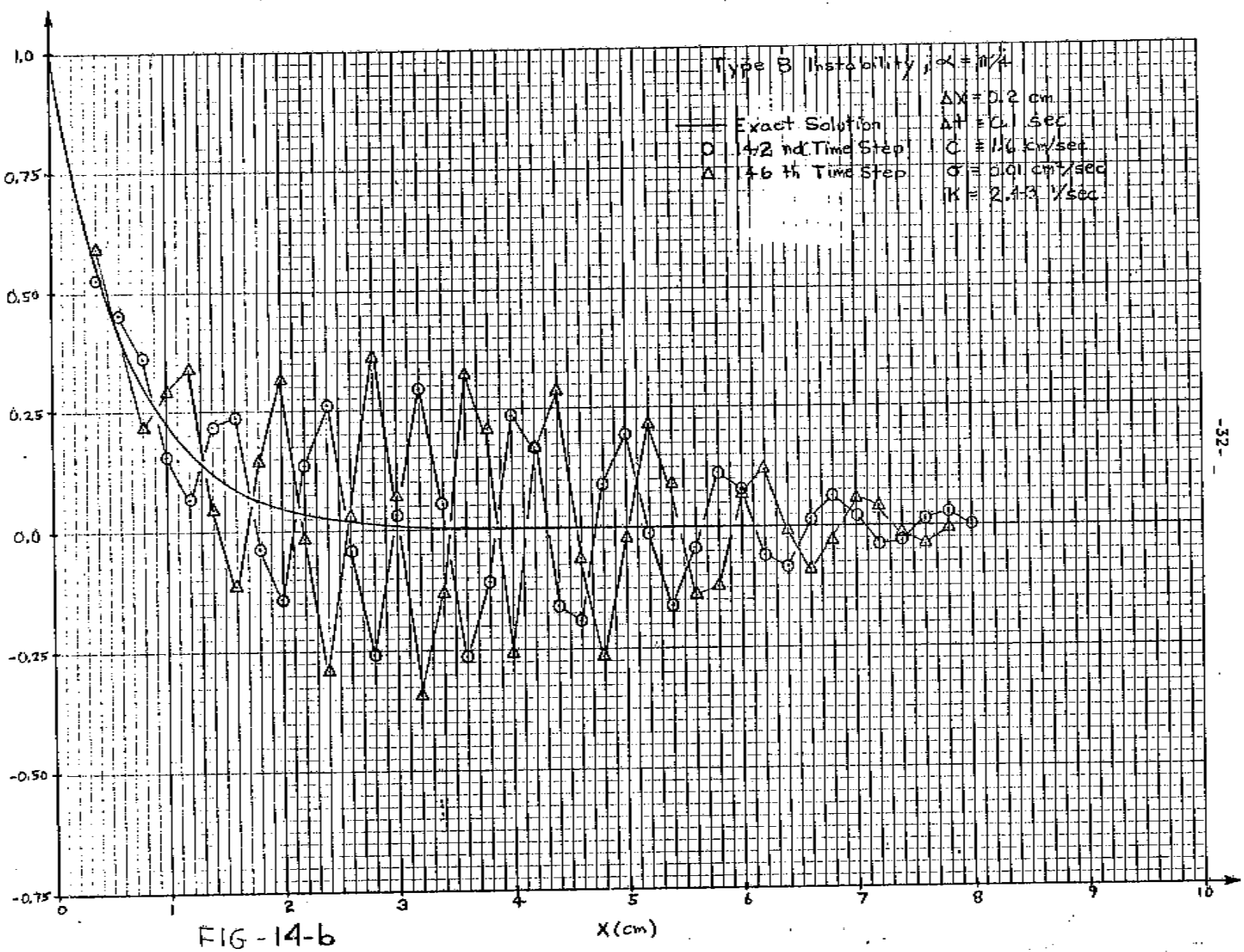

FIG-14-b

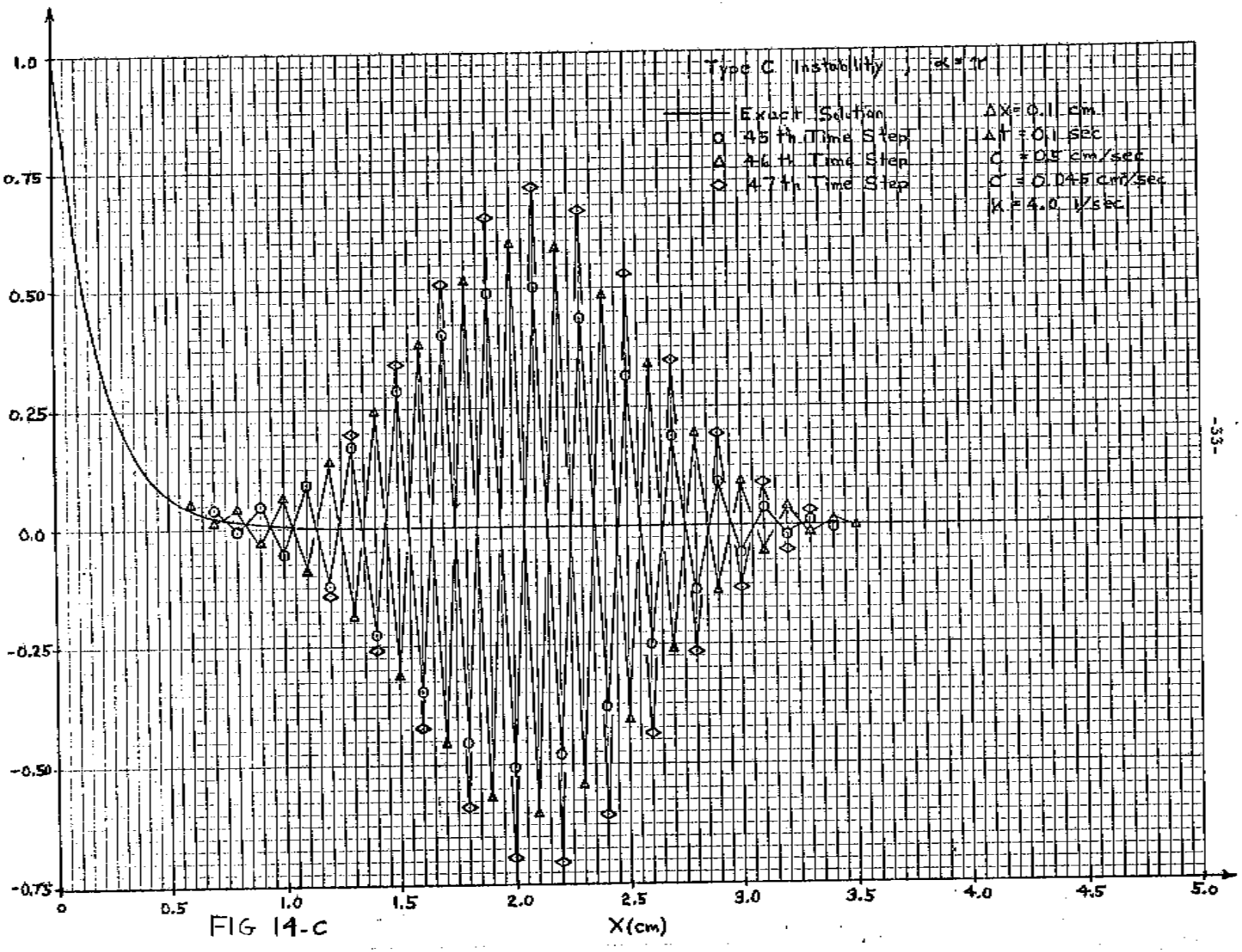

FIG 14-C

REFERENCES

[1] Brillouin, L. (1960) "Wave Propagation and Group Velocity" Academic Press Inc. New York, N.Y.

[2] Hildebrand, F.B. (1968) "Finite Difference Equations and Simulations", Prentice Hall Inc.

[3] Richtmyer, R.D. and K.W. Morton (1967) "Difference Methods for Initial Value Problems" Interscience Publishers, New York, N.Y.

[4] Roache, P.J. (1972) "Computational Fluid Dynamics" Hermosa Publishers, Albuquerque, N.M.

[5] Vichnevetsky, R. and A.W. Tomalesky (1971), "Spurious Wave Phenomena in Numerical Approximations of Hyperbolic Equations", Proceedings, Fifth Annual Princeton Conference on Information and Systems Science, March.

[6] Vichnevetsky, R. (1972) "Stability Charts of Methods of Lines for Partial Differential Equations" Proceedings, Sixth Annual Princeton Conference on Information Science and Systems. Princeton University, March 1972.